Geophysical Research Letters

Supporting Information for

Platelet Ice under Arctic Pack Ice in Winter

Christian Katlein[1*], Volker Mohrholz[2], Igor Sheikin[3], Polona Itkin[4], Dmitry V. Divine[5], Julienne Stroeve[6,7], Arttu Jutila[1], Daniela Krampe[1], Egor Shimanchuk[3], Ian Raphael[8], Benjamin Rabe[1], Ivan Kuznetov[1], Maria Mallet[1], Hailong Liu[9], Mario Hoppmann[1], Ying-Chih Fang[1], Adela Dumitrascu[10], Stefanie Arndt[1], Philipp Anhaus[1], Marcel Nicolaus[1], Ilkka Matero[1], Christian Haas[1]

[1]Alfred-Wegener-Institute Helmholtz Center for Polar and Marine Research, Bremerhaven, Germany

[2]Institut für Ostseeforschung, Warnemünde, Germany.

[3]Arctic and Antarctic Research Institute, St.Petersburg, Russia

[4]UiT University of Tromsø, Tromsø, Norway

[5]Norwegian Polar Institute, Tromsø, Norway

[6]University College of London, London, United Kingdom

[7]Center for Earth Observation Science, Department of Environment & Geography, University of Manitoba, Winnipeg, MB, Canada

[8]Thayer School of Engineering, Dartmouth College, Hanover NH, United States of America

[9]Shanghai Jiao Tong University, Shanghai, China

[10]University of Gothenburg, Gothenburg, Sweden

Contents of this file

Introduction

This supplementary information provides additional graphics – mostly images – to further illustrate the platelet ice observations described in the main paper. All raw data used in this study are archived in the MOSAiC Central Storage (MCS) according to the MOSAiC Data Policy at the Alfred-Wegener-Institute (AWI) and will be accessible unrestricted after the 1 Jan 2023.

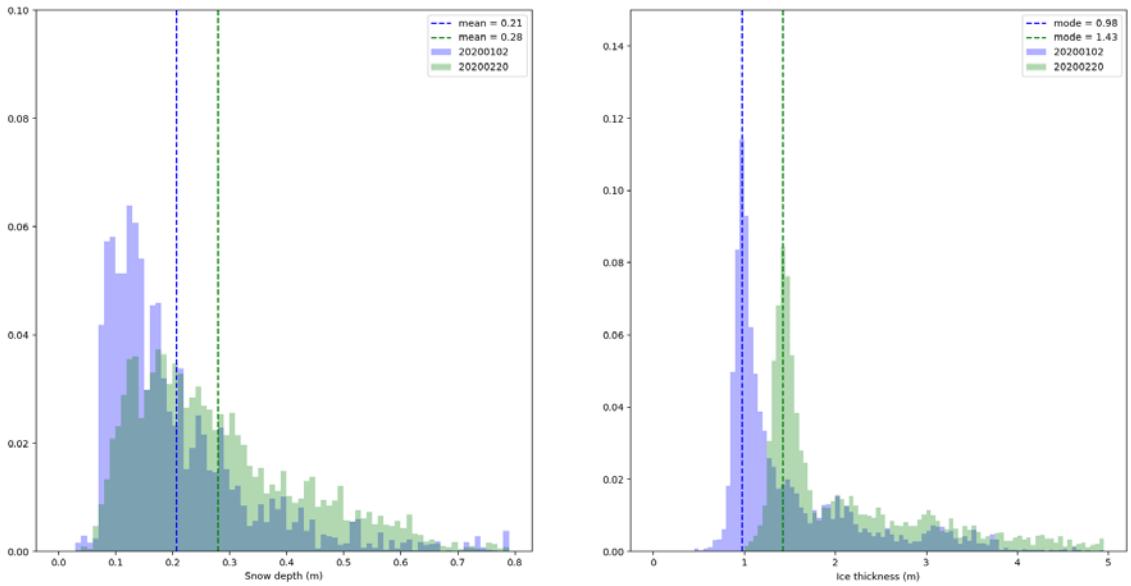

Figure S1. Snow (left) and ice thickness (right) distributions as measured by a Magna Probe (Snow Hydro) and an electromagnetic device GEM-2 (Geophex) on the two main transect loops on the MOSAiC floe. Blue colors indicate a survey from 2 January 2020 coinciding with the first platelet ice observations, while green colors represent the situation on 20 February 2020. Data provided by Stefan Hendricks, AWI.

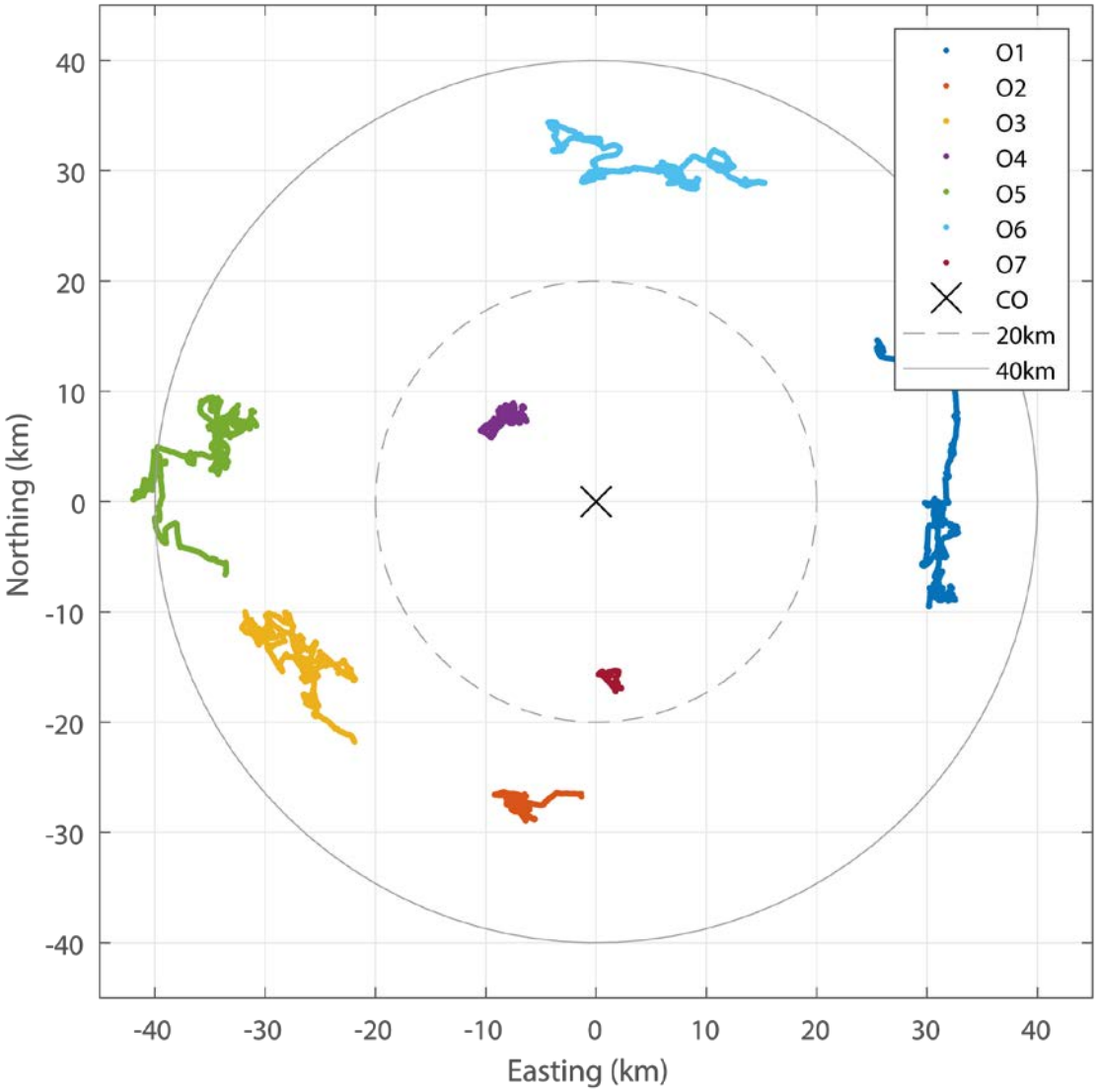

Figure S2. Relative locations of oceanographic autonomous observatories (O1-O7) in relation to the MOSAiC central observatory (CO). Plot is corrected for apparent rotation, as the MOSAiC floe drifts across a wide range of latitudes.

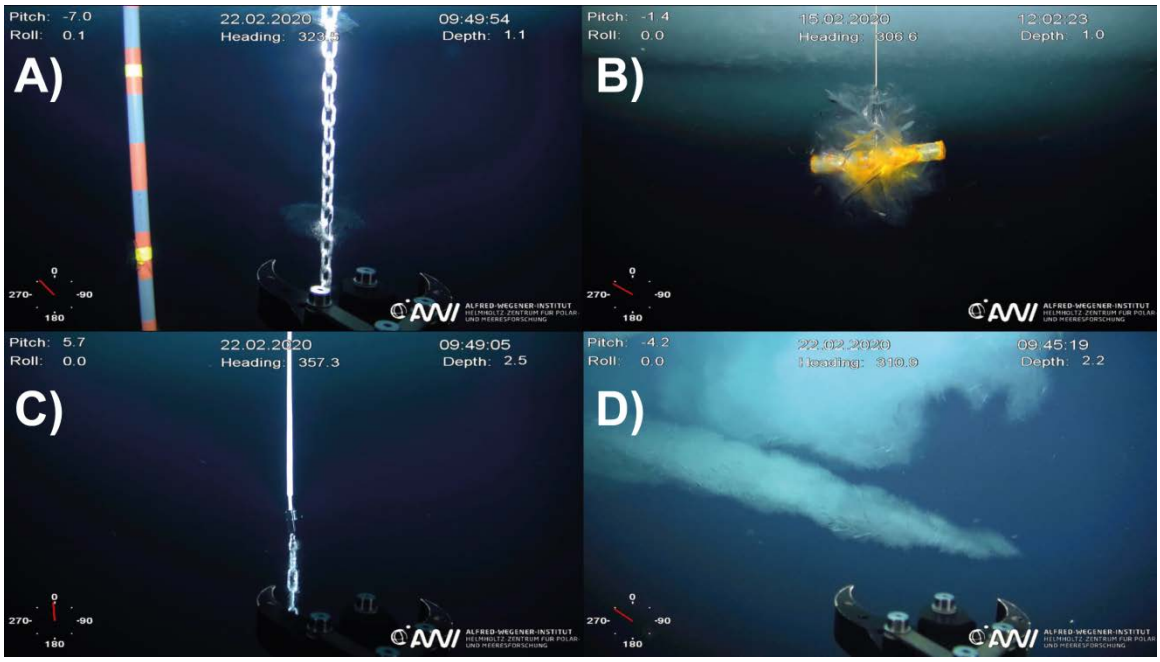

Figure S3. A) A 12 cm large single platelet crystal intergrown into a stainless steel chain. B) Platelet crystals growing around the 20cm long steel cross-bar of a hot-wire. C) Thermistor chain covered in polymer heat-shrink. Note the absence of platelet ice on the plastic surface. D). Platelet crystals growing on an extended spike without any shelter from strong currents.

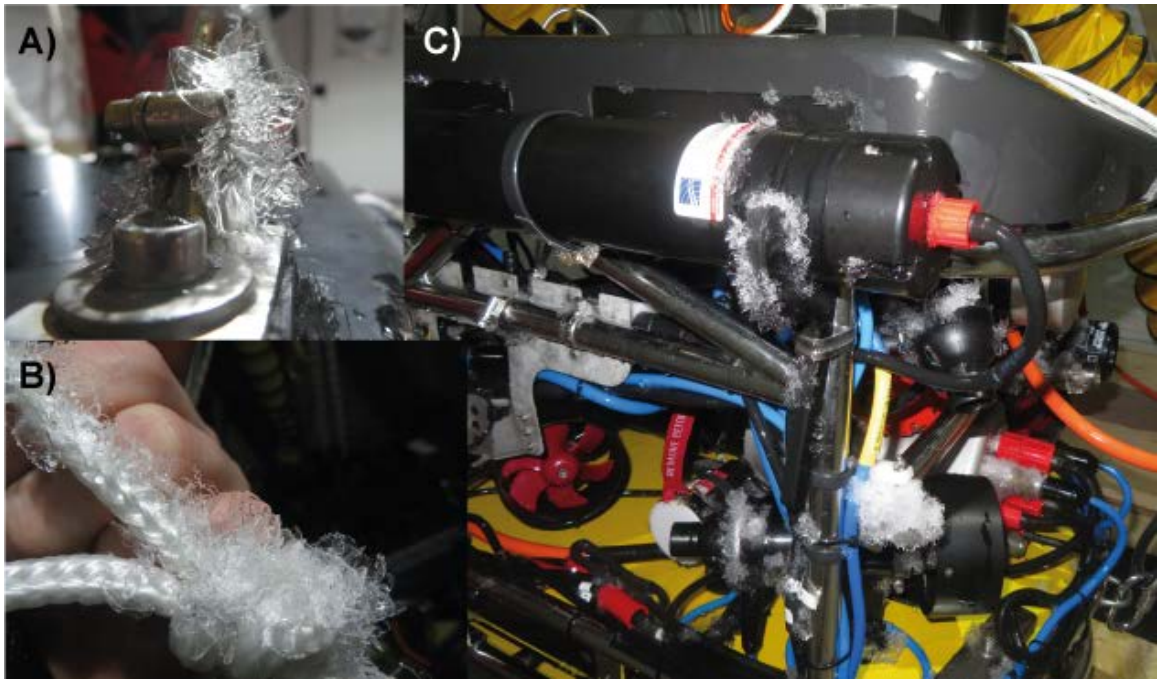

Figure S4. Platelet ice crystal growth on the ROV system: A) Close-up of small crystals on the ROV, B) Crystals growing on the attachment rope. C) Platelet growth on the edges and corners of the ROV system.

Figure S5. Vertical gradient of platelet ice growth on a chain.

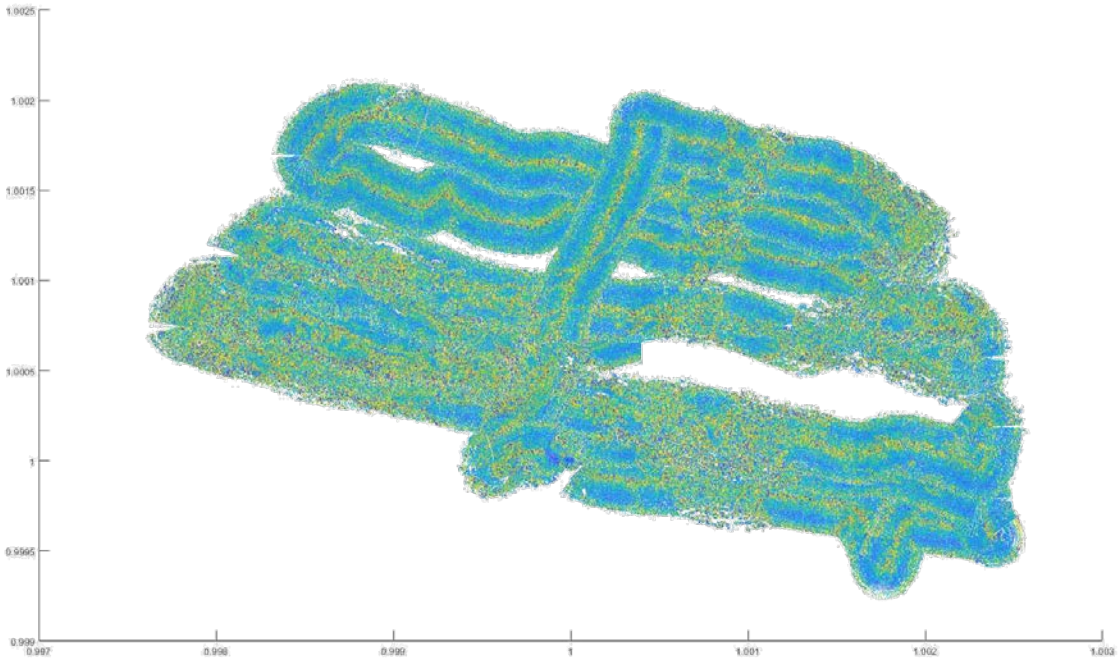

Figure S6. Map of raw acoustic backscatter intensity measurements. Data are not corrected for across-track incidence angle differences. Regions of generally elevated backscatter are co-located with ridges (see Figure 1).

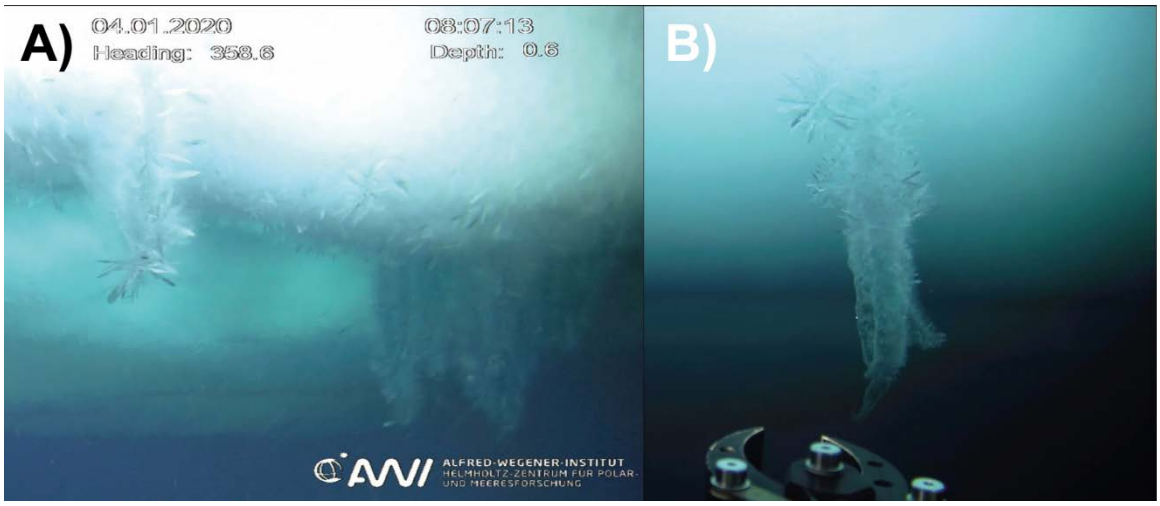

Figure S7. Brinicles under the ice observed surrounded with (A) and without (b) extensive platelet ice coverage.

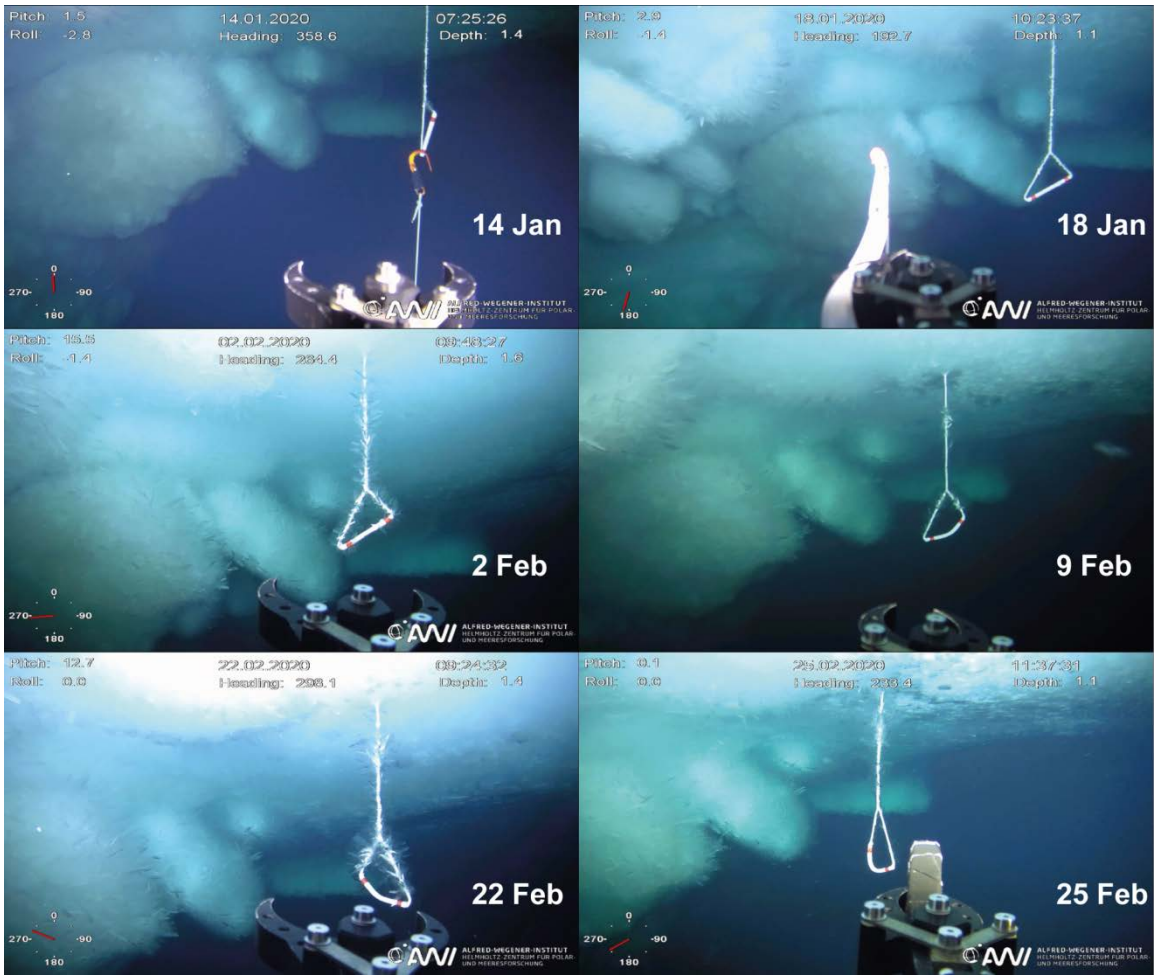

Figure S8. Time series of under-ice photographs showing the development of platelet ice on ridge blocks and a rope sling deployed next to the ridge observatory.

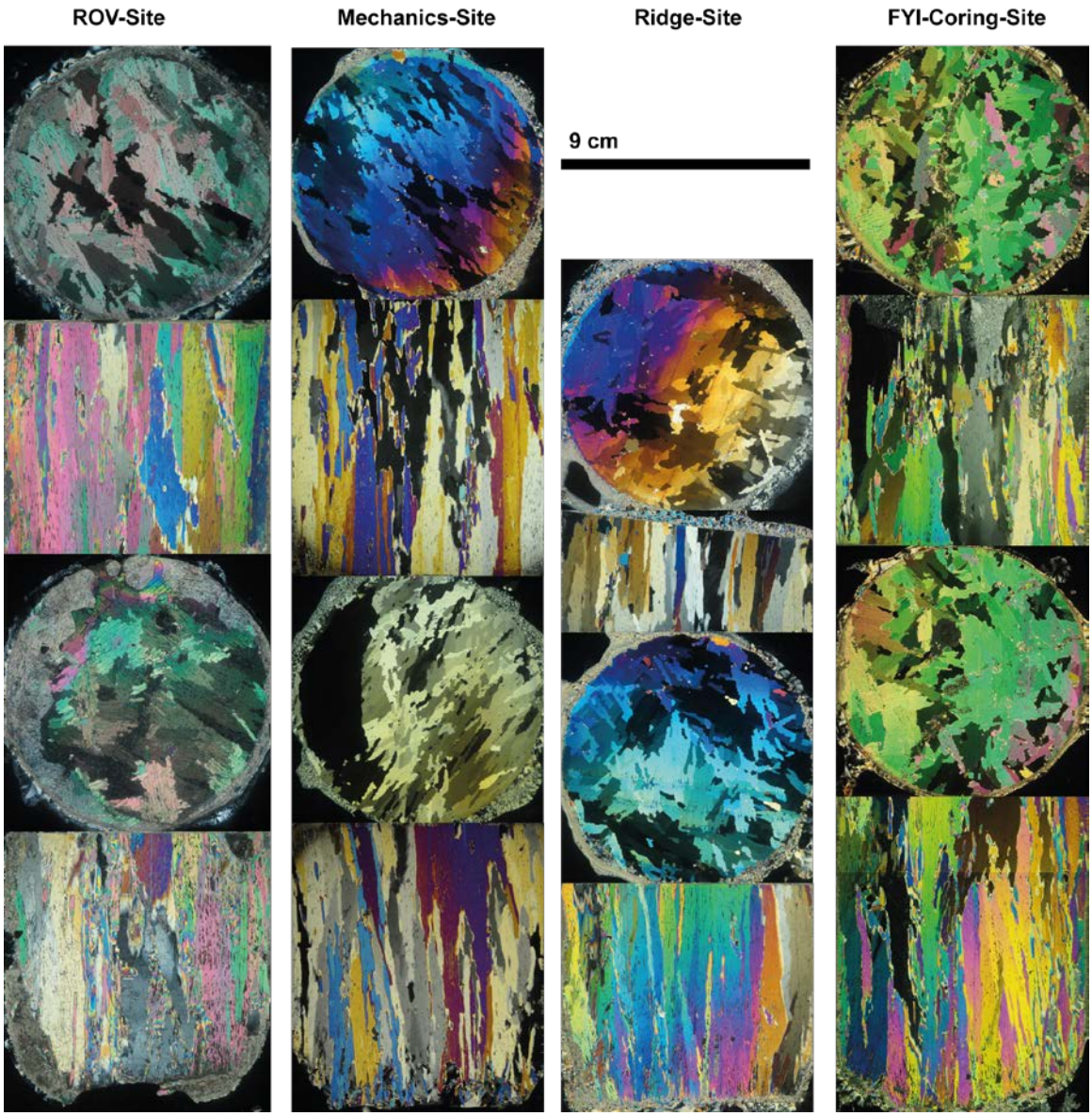

Figure S9. Thin sections of ice cores taken in the end of February photographed between crossed polarizers: horizontal (circular) and vertical thin sections of the two bottommost segments of retrieved ice cores on second year ice (thickness 1.8m) near the ROV deployment site (left), second year ice (thickness 1.27m) at the mechanics site (left middle), first year ice next to the ridge observatory site (thickness 1.2m, right middle), as well as first year ice (thickness 1.23m) at the coring site (right). Site locations are depicted in Figure 1, except the first year ice coring site which lies about 2 km away.

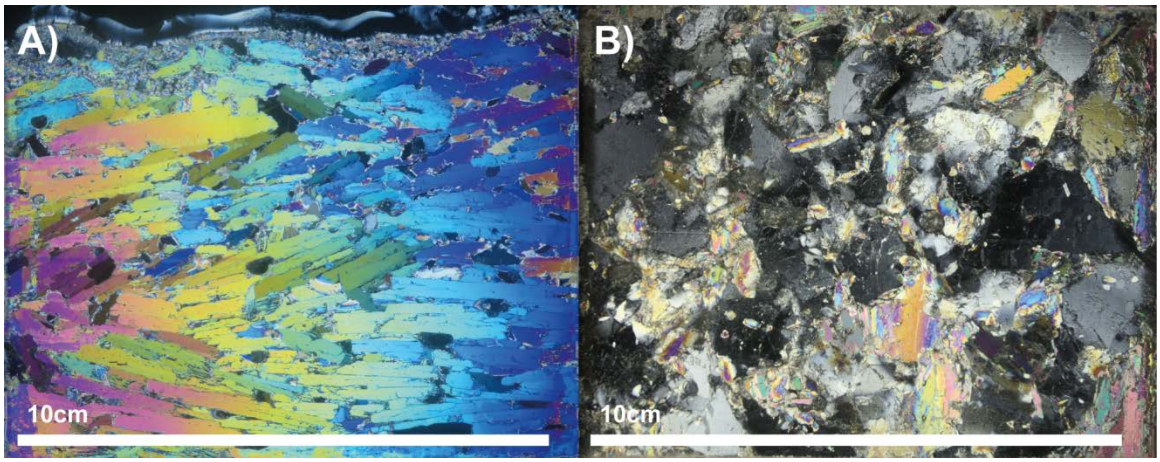

Figure S10. Thin sections of ice platelets collected with the ROVnet and refrozen with seawater in a styrofoam box photographed under crossed polarizers: A) vertical thin section showing individual platelets from the side. B) horizontal thin section showing that c-axis orientation is mostly normal to the platelet.

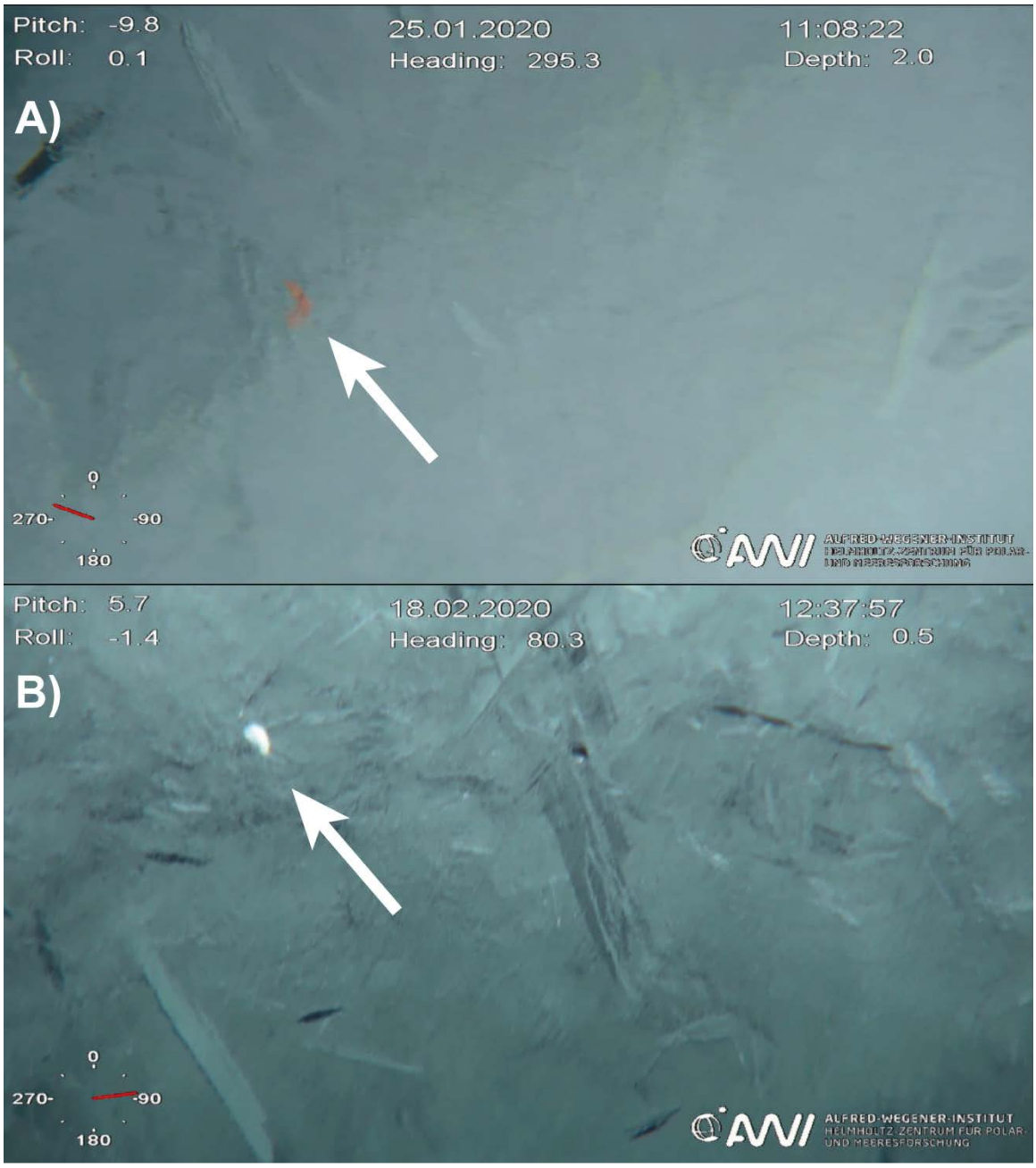

Figure S11. A&B) Under-ice macro fauna – probably amphipods – roaming in between the ice platelets.

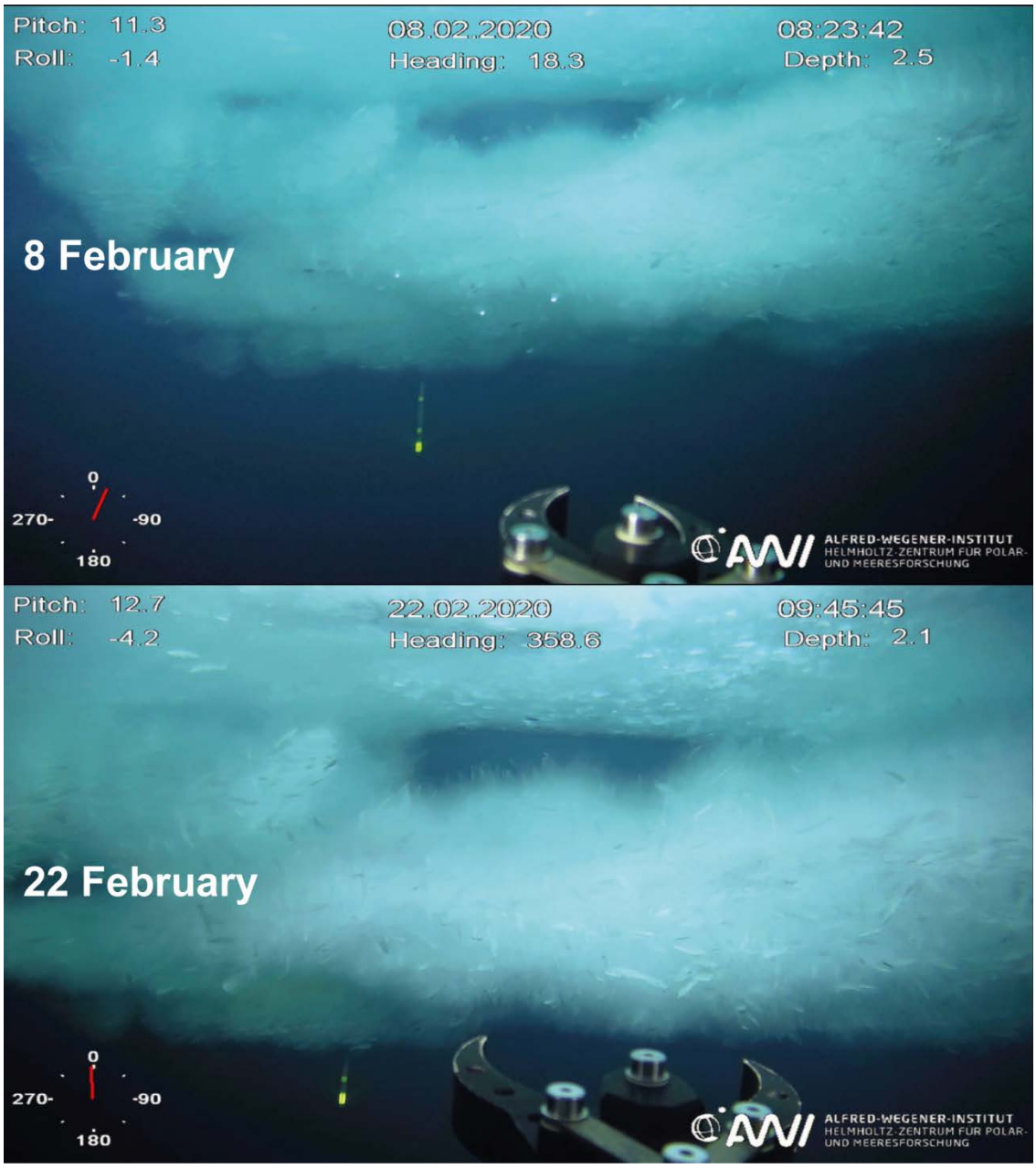

Figure S12. Time series of under-ice photographs showing the development of "upward-growing" platelet ice on top of a rafted floe.

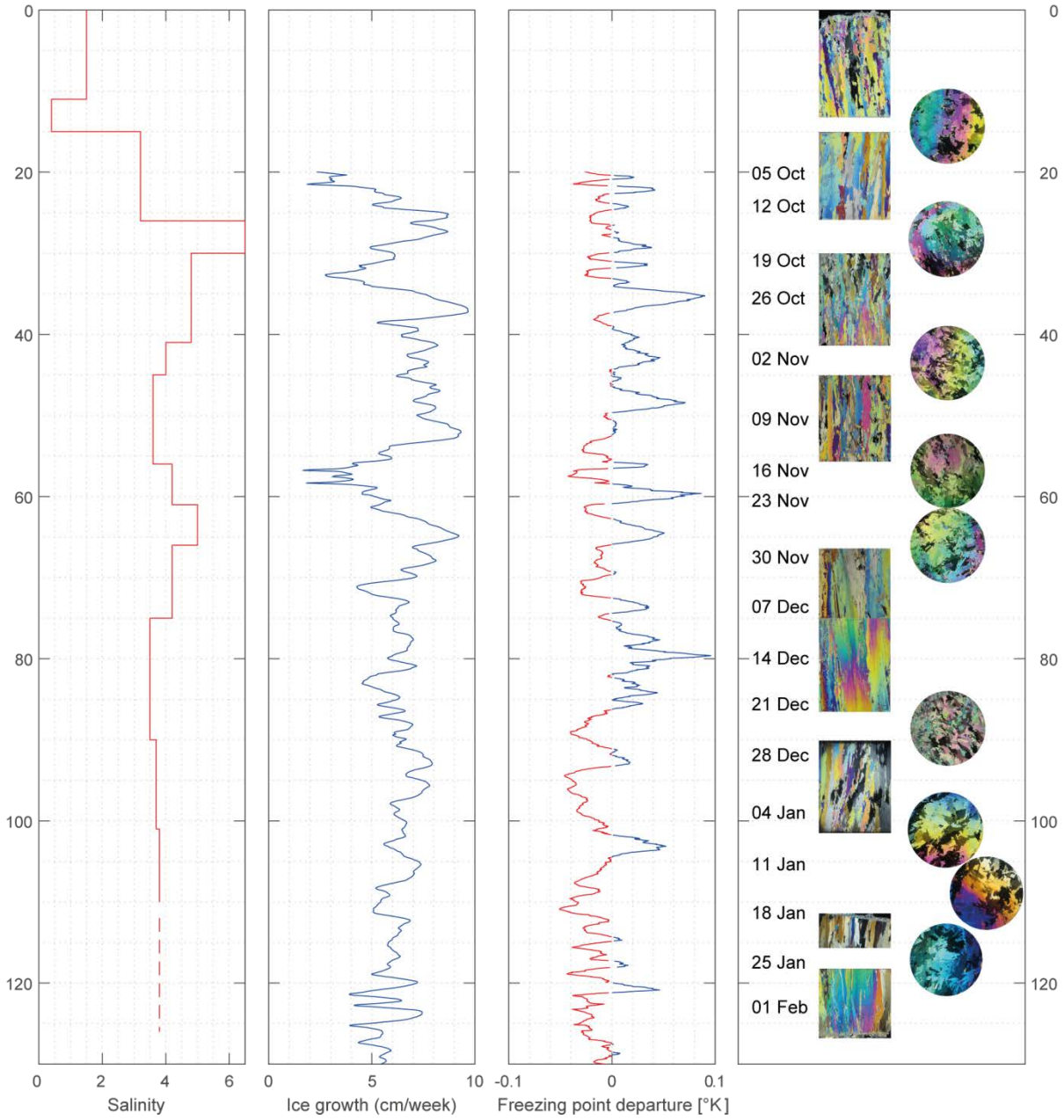

Figure S13. Analysis of the ice core retrieved on level first year ice / residual ice in the ROV survey area next to the ridge observatory. Bulk salinity (left), ice growth derived from a thermodynamic model (left middle), freezing point departure as derived from the ship's thermosalinograph. Thermosalinograph temperatures have been adjusted arbitrarily, so the shown freezing point departure is only meant as a temporal proxy of super-cooling and not absolutely calibrated (right middle). Vertical (rectangular) and horizontal (circular) thin sections along with ice formation date according to the thermodynamic model (right).